NORTHERN CALIFORNIA GEOLOGICAL SOCIETY

Field Guide to the Unique Geology/Geochemistry of Ring Mountain Open Space Preserve (RMOSP) Marin County, CA

Saturday, May 19, 2018

Field Trip Leaders:

William E. (Bill) Motzer, PhD, PG, CHG, CPG
Geologist/Geochemist

Mark Petrofsky
NCGS Outreach Coordinator

Cover: View southwest of Ring Mountain exotic block terrain, including *Turtle Rock* (loaded with school children) – largely composed of blueschist. Marin Headlands in distance. October 2017 photo.

Field Guide to the Unique Geology/Geochemistry of Ring Mountain Open Space Preserve (RMOSP) Marin County, CA

Contents

Introduction

Background

This guide book is an expansion of a "mini" field guide developed for the American Institute of Professional Geologists (AIPG) U.C. Davis and Sonoma State University combined student's chapter field trip, led by the authors on May 14, 2016. However, earlier NCGS field trips led by Dr. John Wakabayashi in 2001 (*Breweries and Blueschists*), Dr. Dave Bero in 2004 and again Wakabayashi's *Breweries and Blueschists II* introduced us to the wonders of these rocks (Wakabayashi 2001 and 2004; Day, 2004; Gordon, 2005: updated by Detterman and Garbutt). In May 2015 and April 2016, the authors and John Christian led members of the Contra Costa Hills Hiking Club on Ring Mountain Open Space Preserve (RMOSP) trails mostly to see the rare endemic wildflowers and Native American mortar holes and petroglyphs. Our most recent field trip, on October 27, 2017, was for the Northern California Section of the Professional Environmental Marketers Association (PEMA). This field guide is not intended as a detailed description or explanation of the RMOSP. Instead, it's a generalized summary and, with that in mind, we have included a bibliography of important and popular references describing past and on-going research.

Overview of Serpentinites, Ophiolite, and Ultramafic (UM) Rock Terrains

World-wide, when compared to other rock-types, serpentinites are volumetrically minor. However, they occur in all ancient orogenic belts, particularly in ancient subduction and suture zones. When serpentinites occur with other rocks such as felsic and mafic volcanic basalt, UMs (e.g., harzburgite or peridotite) and minor chert, the suite is collectively named an *ophiolite* (**Figure 1** and **Figure 2**). These rocks occur on all continents, including Antarctica. Approximately greater than (>) about three percent of Earth's surface rocks are composed of serpentinite and serpentinized peridotite (Guillot and Hattori, 2013).

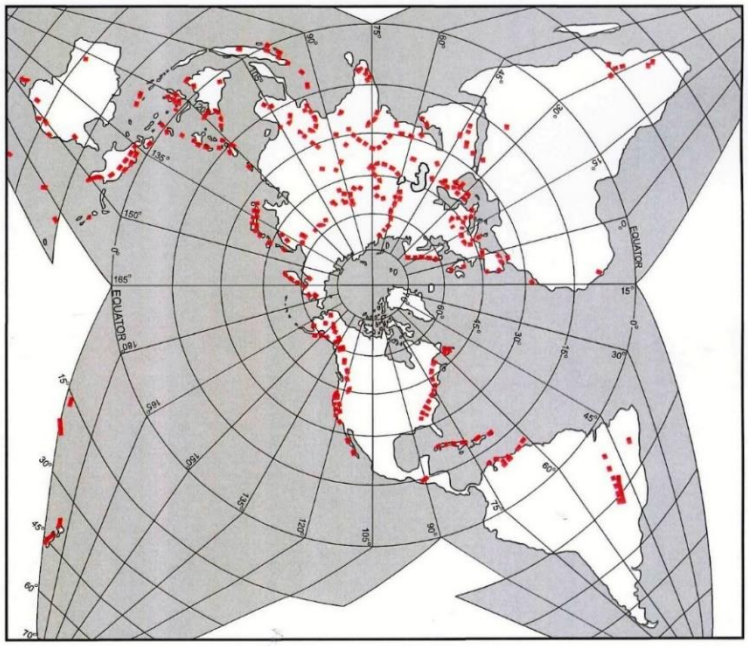

Figure 1: *North polar projection showing world-wide serpentinite and ophiolite distribution (red squares) (Modified from Oze, et al., 2007).*

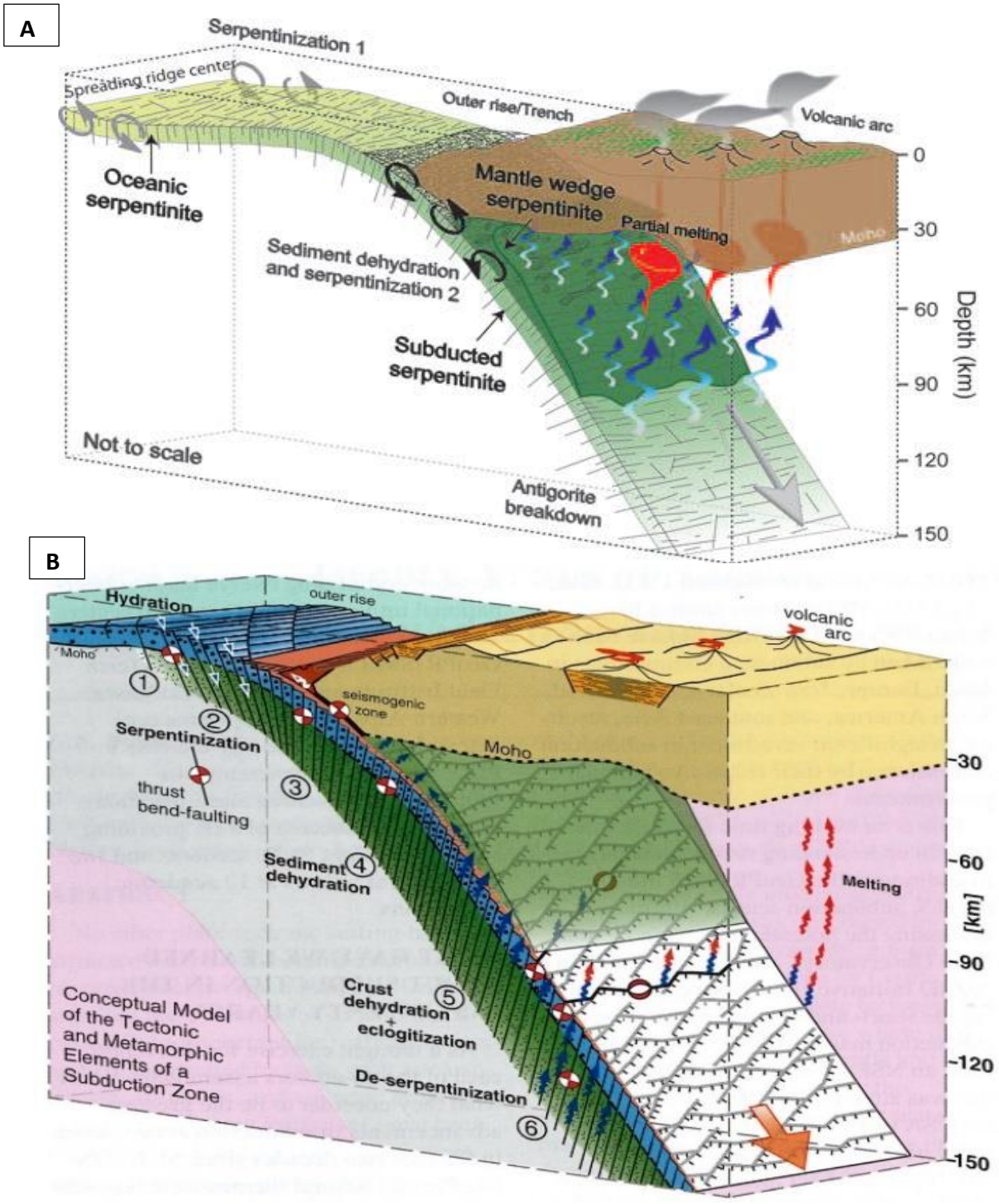

Figure 2: *Conceptual subduction zone-related models showing oceanic slab serpentinization.* ***A****: oceanic and subducted-related serpentinization from Guillot and Hattori (2013).* ***B:*** *fast subduction model from spreading center showing metamorphic evolution (Bebout, et al., 2018).*

The subduction and subsequent obduction of high-pressure and/or ultra-high-pressure rocks results in decoupling of these rocks within the subducting slab (**Figure 3**). This may be associated with deformation and decoupling of the down-going slab (Vogt and Gerya, 2014). However, the average density of the hydrous serpentinite mélange has been calculated to be lower than that of anhydrous mantle peridotite (Hirth and Guillot, 2013). Because serpentinite is more "buoyant" the up-thrusting or obduction results in exhumation along with UM rocks "mixed" with the serpentinized peridotite/harzburgite. exhumation along with UM rocks "mixed" with the serpentinized peridotite/harzburgite.

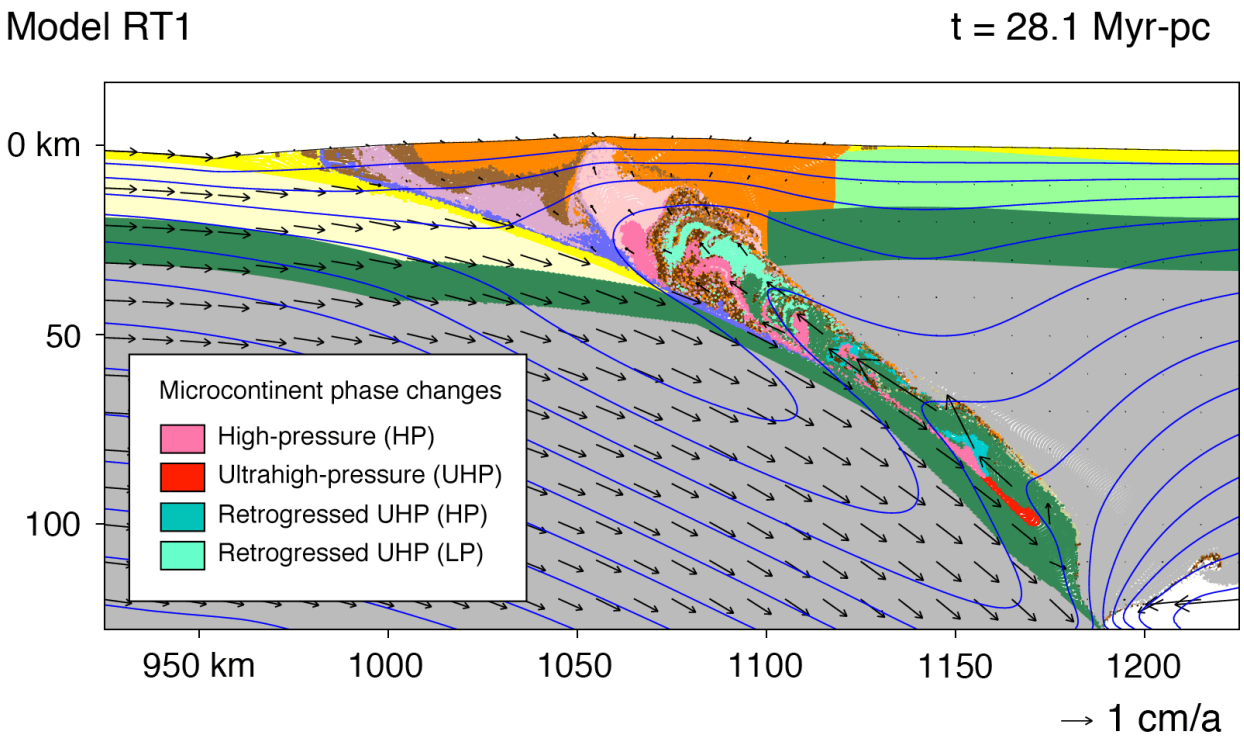

***Figure 3**: Part of an animated model for down-going (subducting) slab (in green) with formation of high pressure (in pink) and ultrahigh pressure (red) rocks and resultant phase changes (regression) of obducted rocks (in blue) (from Butler, et al., 2014).*

A Brief History of Ring Mountain Open Space Preserve (RMOSP)

RMOSP was first occupied by the Coast Miwok indigenous people, who left their visible traces as mortar holes with scattered clam and other shell fragments indicating seasonal occupation to perhaps 2,500 years ago (Ka). RMOSP also contains approximately 25 petroglyph (also known as curvilinear nucleated stone art) sites believed to be 5,000 to 8,000 years old, having been carved by the Miwok Hokan or Penutian-speaking peoples. Such carvings may be related to fertility ceremonies. In 1843, the area became part of a larger Mexican Land grant given to John Reed and it continued to be largely owned and used for grazing cattle by Reed and Deffebach family descendants until 1951 (Hogan, 2008; Marin Conservation League, 2011).

Ring Mountain itself was subsequently named for George Ring, a Marin County Supervisor from 1895 to 1904. In 1951, the U.S. Army leased the land from the Deffebachs, leveled the peak, and constructed roads and barracks, for a four 90-mm anti-aircraft long barrel cannons. The guns were never fired. In the late 1950s and early 1960s, the Army removed all their installations. As the area became more populated, grazing ceased by 1965 and in the 1970s developers began planning for 2,100 houses and apartments across and on top of Ring Mountain. Concerned local citizens, adjacent homeowners, the California Native Plant Society, Marin Audubon Society, the Environmental Forum, and Sierra Club raised funds to save Ring Mountain as open space. Phyllis Ellman of the California Nature Conservancy (CNC) led the movement. In 1984, Ring Mountain was ultimately purchased by the CNC with establishment of a 307-acre environmental resource area under Marin County Open Space District management (Marin Conservation League, 2011).

Ecology

Plants

Serpentine soils are considered as model systems for plant adaptation, speciation, and species interaction study, generally hosting stunted vegetation; however, many plants have locally adapted forming distinctive soil ecotypes (Anacker, 2014). RMOSP hosts at least 75 species of wildflowers of which many are native and unique to RMOSP such as the Oakland Star tulip (*Calochortus umbellatus*), goldfields, tidy tips, and common buckwheat. In the serpentine barrens, native grasses including serpentine reed grass (*Calamagrostis ophitidis*), bunch grass, and needle grass are interspersed with rare annual flowers such as the Tiburon mariposa lily (*Calochortus tiburonensis*), which is found only on the upper slopes of RMOSP and nowhere else in the world (**Figure 4**). This unique wild flower was discovered in 1972 by Dr. Robert West, a Corte Madera physician and botanist. In shady spots and along creeks, poison oak is ubiquitous, so please be careful on narrow single-track trails (Marin County Parks.org, 2010; Marin Conservation League, 2011).

Animals

Approximately 75 species of butterflies occur, including Anise Swallowtail, Arrowhead Blue, California Sister, and California Tortoiseshell. About 109 species of birds occur including Acorn Woodpecker, Allen's and Anne's Hummingbird, American Crow, American Goldfinch, Barn Owl, and Barn Swallow. Mammals include coyote, mule deer, and perhaps fox and bobcat (Marin County Parks.org, 2010).

Figure 4: *Protected areas occur on RMOSP to preserve rare endemic species such as the Tiburon mariposa lily (on right). April 2016 photo.*

Geology

The greater San Francisco Bay area has some of the complex geology of any area worldwide (**Figure 5**). Rocks range from unaltered to slightly metamorphosed Franciscan Complex/mélange to complex and high grade metamorphic rocks at RMOSP and other San Francisco Bay localities. Franciscan Complex/mélange rocks are prominent in the Marin Headlands (Elder, 2013) where graywacke (lithic sandstones), oceanic basalt flows (including pillow basalts), and radiolarian chert, initially deposited on and into the deep ocean floor at and adjacent to equatorial oceanic spreading ridges were subsequently subducted under the North American plate beginning perhaps 160 to 140 million years ago (Ma).

Metamorphism and Metamorphic Age Determination

At RMOSP, the rocks have undergone considerably more intense metamorphism resulting from heat and pressure at approximate depths ranging to perhaps greater than 300 km. These rocks have been brought to the surface by obduction – the subducting serpentinized plate being scraped off and onto the adjacent continental plate forming distinctive terrains separated by low angle thrust faults (Bero, 2014; Wakabayashi, 2017). As previously indicated, these rocks rose buoyantly to the surface, or, in the case of the exotic blocks (aka: *knockers*) were carried along with the more buoyant rocks. For the Franciscan, metamorphic facies related to temperature and pressure (depth) are shown on **Figure 6** (Raymond, 2017). Wakabayashi (2013) described, summarized, and estimated metamorphic pressures for high-grade

metamorphic rocks ranging from approximately (~) 5 kilobars (kbar) for the lowest-pressure amphibolites to 20 to 25 kbar for eclogites. Lower-grade blueschist rocks were created at pressures of ~6 to >10 kbar and sub–blueschist grade rocks were metamorphosed at pressures of 4 kbar or less. Metamorphic ages of Franciscan rocks generally approximate the time of subduction, because exhumation of these rocks occurred while subduction and "refrigeration" (i.e., retrograde metamorphism) were ongoing (Ernst, 1988; Wakabayashi 2013).

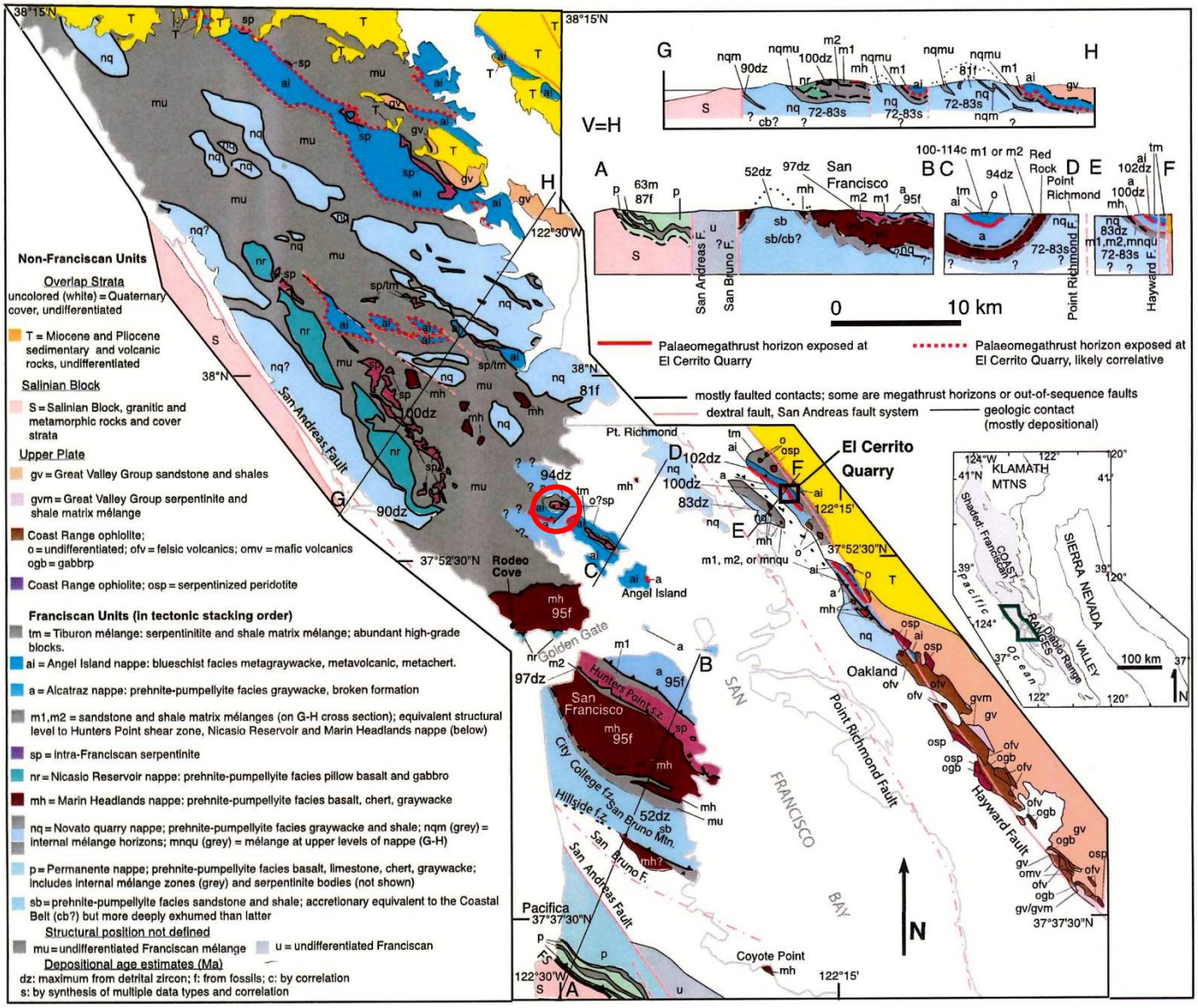

Figure 5: *Geology of Franciscan Complex in the San Francisco Bay area showing the structural relationships between nappes (Wakabayashi and Rowe, 2015). Red circle shows the location of RMOSP.*

Wakabayashi and Dumitru (2007) obtained hornblende ages of about 156 and 159 Ma, respectively, from high-grade amphibolite blocks from San Francisco's McLaren Park and the Hunters Point Shear Zone. A lawsonite [hydrous calcium-aluminum silicate or $CaAl_2Si_2O_7(OH)_2 \bullet H_2O$] lutetium-hafnium isotope ($^{176}Lu/^{177}Hf$) geochronometer age determination for RMOSP rocks indicates 145.5 Ma for lawsonite-blueschist facies metamorphism (Mulcahy, et al.,2009).

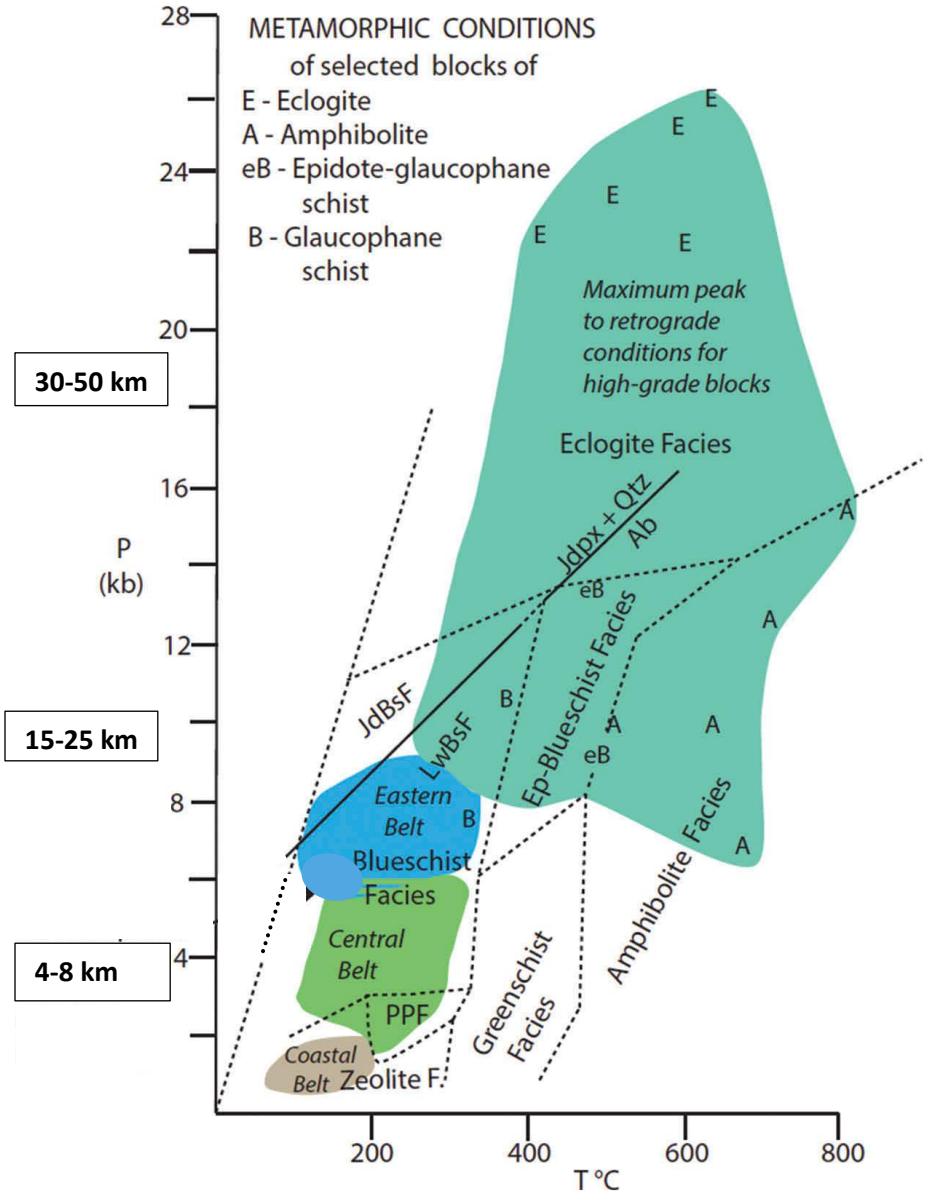

Figure 6: *Metamorphic facies diagram applicable to the Franciscan showing temperatures of formation (bottom), pressures (left side and depths (added) (modified from Renner, 2017; MacKinnon, 2018 and personal communication).*

Structure

Wakabayashi (2013) described the geology and structure of RMOSP as follows:

> *The geology of Ring Mountain consists of several folded nappes. Variably serpentinized harzburgite without exotic blocks makes up the highest nappe. Serpentine minerals in this nappe appear to be entirely or predominantly lizardite with some chrysotile. Structurally beneath this unit, there is a serpentinite matrix mélange with a variety of metamorphic blocks. The mélange matrix, consisting of serpentinite sandstone, breccia, and conglomerate with exotic sand- and gravel-sized clasts, has itself been recrystallized, with growth of antigorite and possibly talc and/or tremolite. It is not clear whether the latter occur here as true neoblastic minerals (postdating sedimentation of serpentinite debris); they are common in detrital clasts.*

Wakabayashi includes RMOSP as part of the Tiburon mélange that overlies the Alcatraz nappe in which the rocks are largely of blueschist facies (**Figure 5,** cross section C-D). These are also exposed at the El Cerrito quarry (cross section E-F) as the eastern limb of a NE-SW trending synform that may control San Francisco Bay's structure (cross section A-B).

General RMOSP Lithology

Except where noted, rock types (described largely after Stoffer, 2002) that can be observed in RMOSP and along the field trip route (**Figure 7** and **Figure 8**) include:

- *Graywacke* (German *grauwacke*, signifying a grey, earthy rock), applies to a dark, firmly indurated, coarse-grained sandstone to siltstone composed of poorly sorted angular to subangular quartz and feldspar with dark rock and other mineral fragments, embedded in a compact clayey matrix. Graywacke also suggests an origin environment for rocks deposited adjacent to tectonically active plate margins where rivers draining volcanic island arc terrain deposited substantial amounts of poorly sorted sediments into adjacent ocean basins. Graywackes commonly have graded bedding (layers containing coarse-grained sand at the base and finer-grained mudrock on top) deposited by submarine turbidity currents. Graywacke occurs in the lower elevations of RMOSP but not in the field trip route.
- *Chert* (aka radiolarian chert) typically occurs as red, gray, green, brown, and black varieties. It commonly occurs as a compact, very fine-grained rock having blocky to conchoidal fractures. In outcrop, chert forms layers with thin shale partings or separations, indicating original formation from biogenic ooze buildup by siliceous plankton (*Radiolaria*) casts deposited on the deep ocean floor, generally distant from terrigenous sediment sources. Thin shale partings may represent periods when atmospheric continental dust was periodically blown into the deep ocean, or alternatively, they represent cyclic periods when radiolarian productivity declined. Not all chert has such distinctive layering. The primary mineral component silica (SiO_2), is relatively soluble and therefore mobile under hydrothermal and metamorphic conditions. Jasperized chert most likely represent some type of hydrothermal activity (Snyder, 1978). Along the field trip route chert occurs on top of Ring Mountain having been quarried elsewhere and presumably brought in by the Army Corps of Engineers as road base.
- *Serpentinite:* a metamorphic rock composed of one or more (up to 20) serpentine group rock-forming minerals that are predominantly hydrous magnesium iron phyllosilicates [e.g., $(Mg,Fe)_3Si_2O_5(OH)_4$)],

containing trace to minor amounts of other elements including chromium (Cr), manganese (Mn), cobalt (Co) or nickel (Ni). Because of admixtures, such varieties are not always easy to characterize in hand specimen, and distinctions are not usually made. Three important minerals: antigorite, chrysotile, and lizardite are formed by the *serpentinization*, a hydration and metamorphic transformation of mafic and UM rocks. There is some recent evidence suggesting that deep ocean microbial communities contribute or participate in the hydrogen generating reactions that convert UM to serpentinite in the following reaction for olivine (Templeton, 2011):

$$Mg_{1.8}Fe_{0.2}SiO_4 + 1.37H_2O \rightarrow 0.5Mg_3Si_2O_5(OH)_4 + 0.3Mg(OH)_2 + 0.067Fe_3O_4 + 0.067H_2$$

(olivine) (serpentine) (brucite) (magnetite)

Serpentinization is important at sea floor and tectonic plate boundaries, particularly at subduction zones (Evans, et al., 2013; Guillot and Hattori, 2013, Bebout, et al., 2018; also see **Figures 1** and **2** above).

- *Serpentinized harzburgite* (peridotites). Structurally, the different rock types at RMOSP are separated by thrust faults with the highest units as serpentinized harzburgite with entrained exotic blocks of variable metamorphic grades (i.e., greenschist, blueschist, and eclogite) and the lowest units including blueschist and metagraywacke. At RMOSP, these exotics occur as mafic blocks in serpentinite matrix. An example is "Turtle Rock", which is largely composed of a garnet amphibolite nearly completely overprinted in most areas by blueschist facies. Faulting, tight folds, and imbrications resulted in a blueschist mafic and meta-UM schist (composed of tremolite/actinolite + phengite + chlorite repetitions). Similar characteristics occur in other blocks in this mélange. blocks and are believed to predate incorporation into the clastic serpentinite matrix. Other exotics (e.g., "Climbing Rock") are composed of felsic metavolcanics with remnant tuffaceous breccias and pillow basalt (Bero, 2014; Wakabayashi, 2013 and 2017).
- *Blueschist* is formed by metamorphism of basalt and similar rocks at high pressures and low temperatures, corresponding to depths of 15 to 30 km and temperatures of 200 ^{o}C to ~400 ^{o}C. The rock's blue color is from the predominant minerals glaucophane [$Na_2(Fe,Mg)_3Al_2Si_8O_{22}(OH)_2$] and lawsonite [$CaAl_2Si_2O_7(OH)_2{\cdot}H_2O$].
- *Greenschists* form under temperatures and pressures usually produced by regional metamorphism, typically around 150 to 400 °C and 1.0 to 6 kbar (~4 to 20 km). Greenschists generally have abundant green minerals such as chlorite [$(Mg,Fe)_3(Si,Al)_4O_{10}(OH)_2{\cdot}(Mg,Fe)_3(OH)_6$], serpentine, and epidote [$Ca_2Al_2(Fe^{3+}Al)(SiO_4)(Si_2O_7)O(OH)$], and platy minerals such as muscovite and platy serpentine. Common minerals include quartz, orthoclase feldspar, talc, carbonate minerals and amphiboles (e.g., actinolite).
- *Eclogite*: a metamorphic rock, began as an oceanic basalt that was transformed at pressures found at >35 km depth and temperatures >300 to 600 °C (high-pressure, medium- to high-temperature metamorphism). Eclogites have unique mineral compositions largely consisting of almandine-pyrope (red) garnet [generally $Fe_3Al_2(SiO_4)_3$ to $Mg_3Al_2(SiO_4)_3$] in a green matrix of the sodium-rich pyroxene mineral omphacite [$(Ca,Na)(Mg,Fe,Al)Si_2O_6$)]. Eclogites containing lawsonite may occur at the surface, although this mineral was formed at depths between ~45 and 300 km, thereby indicating unusual exhumation processes.

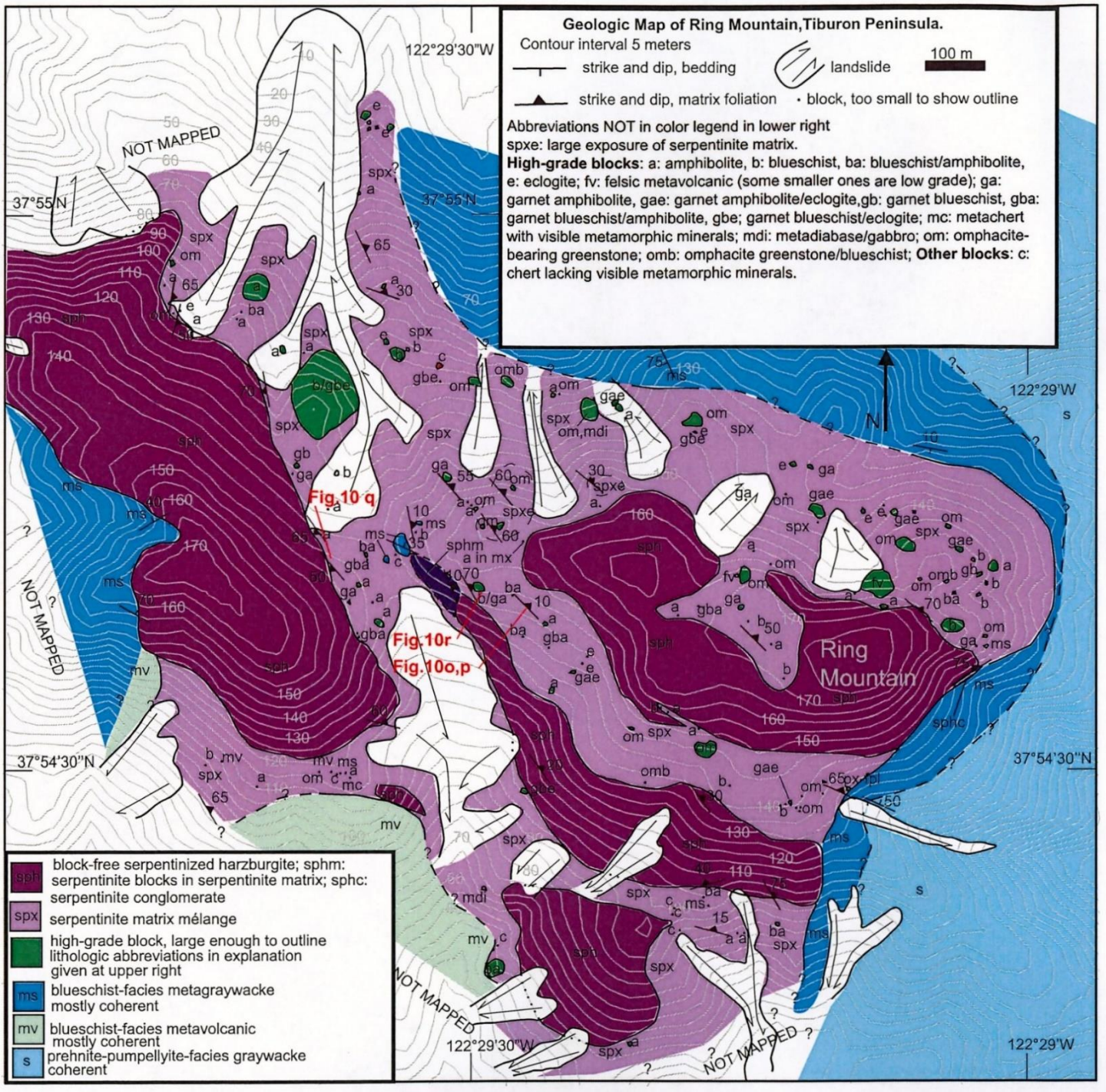

Figure 7: *Ring Mountain Open Space Preserve (RMOSP) Geologic Map (Wakabayashi, 2017).*

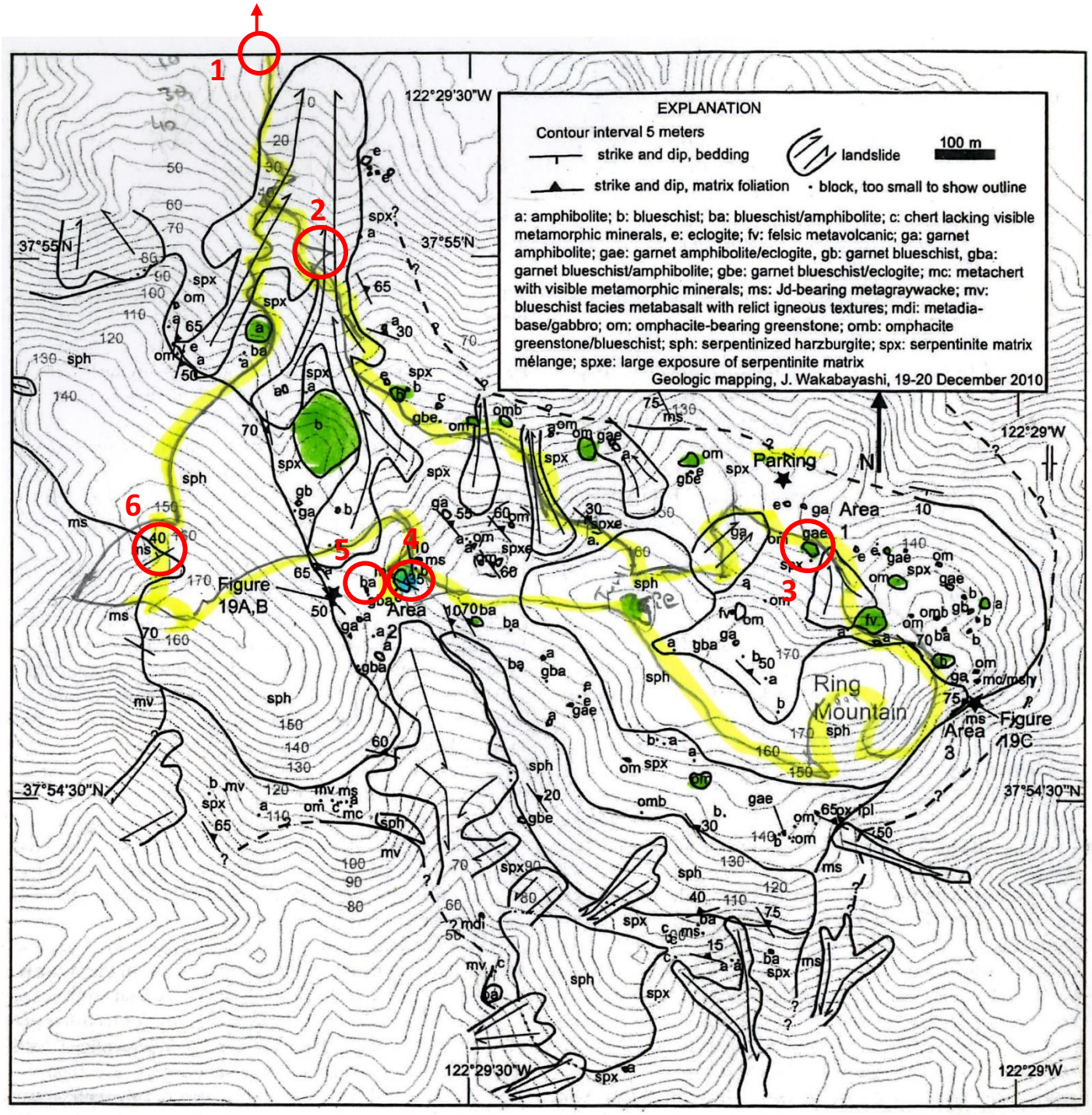

Figure 8: *Ring Mountain Open Space Preserve (RMOSP) trail map with major stops (red circles) overlain on Wakabayashi's 2013 geologic map.*

Pedology

Unique soils, derived from the underlying serpentinite and ultramafic rocks, have very low water-holding capacities. The physical characteristics of soil developing on upland serpentinite include *Henneke Series*, consisting of shallow excessively drained soils with thin stony loamy dark-reddish A (0- to 3-inch-thick) horizons, dark reddish-brown B (3- to 16 inch) horizons and absent C horizons. *Montara Series* soil also form on serpentinite but more so on hillside slopes. These are also well-drained and composed of dark greyish brown clay loam with 0- to 13-inch-thick A horizons and no developed B or C horizons (USDA, 2016).

RMOSP soil types consist of *serpentine-derived soils* toxic to many plants, because of such high nickel, chromium, and cobalt levels (**Table 1**); however, growth of many plants is also inhibited by the low potassium and phosphorous levels and a low calcium/magnesium ratio. Serpentine flora are generally very distinctive, with specialized, slow-growing species and areas of serpentine-derived soil that commonly form shrubland and open, scattered small trees (often conifers) within what would be otherwise densely forested areas. Analyses of shallow (0 to15 cm) serpentine soil samples in northern California indicate nickel and chromium concentrations ranging to 3,900 mg/kg and 10,000 mg/kg, respectively (Kumar and Maiti, 2013). Such soils are generally very stressful for plant growth, consequently forming *serpentine barrens* that may be completely devoid of vegetation but more commonly consist of open grassland or savannas where the climate would normally result in forest growth. S*erpentine barrens* also result in unique eco- or model-systems for evolution, ecology, and conservation studies of rare plant communities (see below and **Figure 9**). On RMOSP serpentine soils and barrens encompass about 225 acres (**Figure 10**).

Table 1: *Nickel and Chromium Concentrations in Serpentinite Terrains (Kumar and Mati, 2013)*

Location/Terrain	Type of Soil/Rock	Depth (cm)	Nickel (mg/kg)	Chromium (mg/kg)
Northern CA	Serpentinite	0-15	1,300-3,900	1,700-10,000
Northern CA	Serpentinite	0-20	6.0-4,955	12.0-5,910
Central Coast Range	Serpentine Grassland	0-20	3,160-3,940	1,650-2,090
	Serpentine Chaparral	—	1,295-2,660	797-1,385

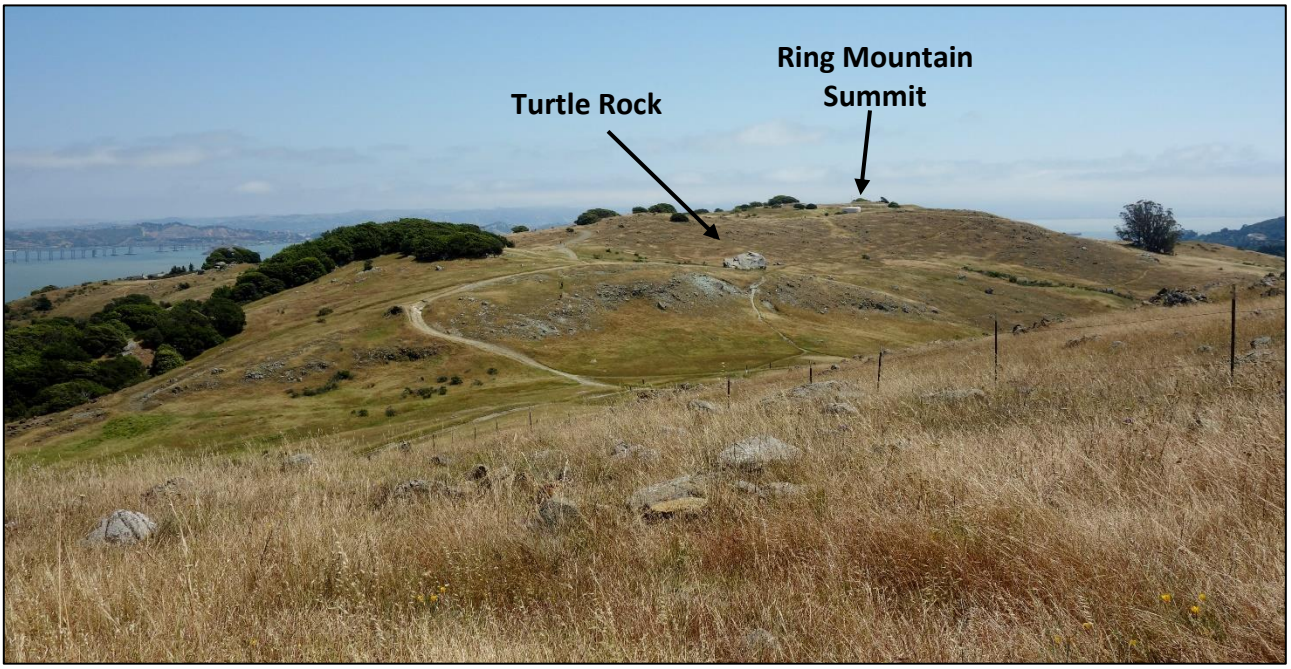

Figure 9: *View back toward Ring Mountain summit and Turtle Rock. Note serpentine barrens with sparse vegetation, mostly grassland with some endemic wild flowers. May 2015 photo.*

Figure 10: *Goggle Earth photo of most of Ring Mountain Open Space Preserve showing the aerial extent of serpentine barrens.*

Geochemistry

Rocks

Ultramafic rocks and serpentinite generally contain chromium(III) [Cr(III)][*] minerals [i.e., Cr oxides: eskolaite (Cr_2O_3)], chromite ($FeCr_2O_4$) and chromium-bearing spinel minerals (e.g., rutile, ilmenite, and magnetite). Some magnetite has been observed by the authors at Stop 6. UMs can average 2,000 milligrams per kilogram (mg/kg or ppm) Cr(III) that may be transformed to Cr(VI) oxyanions [i.e., chromate (CrO_4^{2-}) and dichromate ($Cr_2O_7^{2-}$) in *The Critical Zone* because of geo- and bio-geochemical transformations. Recent reports of Cr(VI) within surface water and groundwater forming from contact with UM rocks, suggest that the overall rate of aqueous Cr(VI) production locally exceeds its retention in solids or reduction to Cr(III) (Guillot and Hattori, 2013; Izbicki, et al., 2015). Particularly interesting are experimental studies showing that manganese oxide minerals [e.g., birnessite (Mn^{IV},$Mn^{III}_2O_4 \bullet 1.5H_2O$)] may act as catalysts transforming Cr(III) to Cr(VI) in groundwater (see groundwater section below) (Motzer, 2005; Priestaf and Rednock, 2015).

Also noteworthy is the abundance of manganese minerals in Franciscan Complex chert. According to Taliaferro and Hudson (1943), Coast Range manganese deposits always occur in the Franciscan and, except for a few rare cases, are always interbedded with red or green radiolarian chert. A small manganese deposit of unknown ore grade, occurring in Red Rock Island's chert, was mined in 1867, with "one schooner full" (about 200 tons) shipped to England (Trask, et al., 1943; Sloan and Karachewski, 2006).

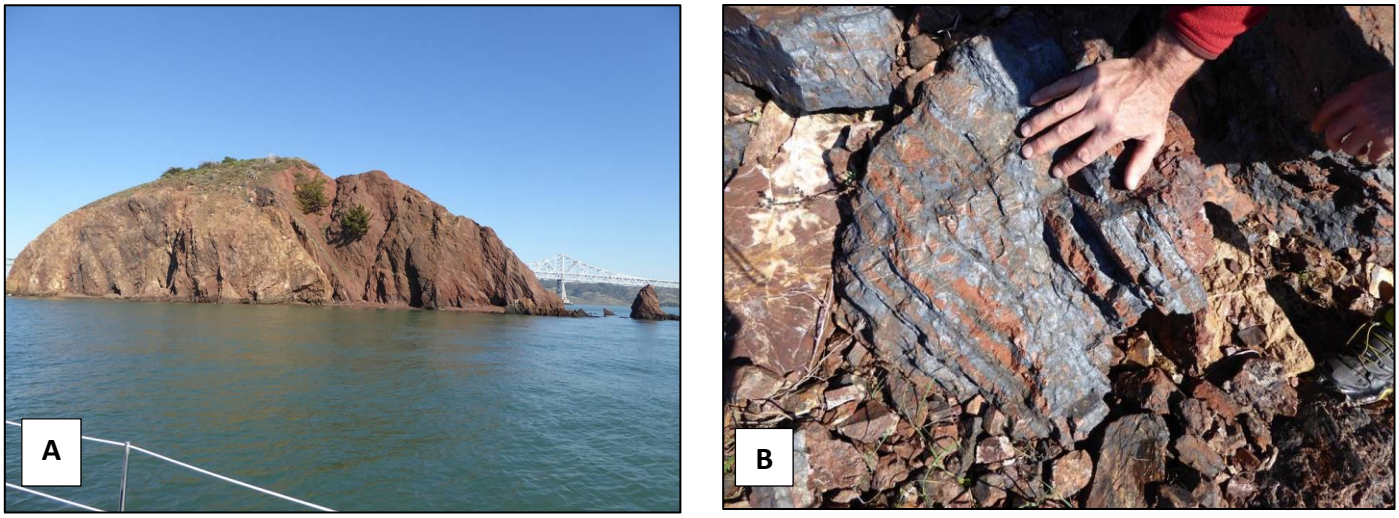

***Figure 11A**: View to northeast of Red Rock (Richmond-San Rafael Bridge in background) in San Francisco Bay. **Figure 14B:** Manganiferous chert occurs on its western side as mapped by MacKinnon (personal communication, 2018). Photos courtesy of Dr. Tom MacKinnon.*

[*] By convention the oxidation state of an element requires using Roman numerals. Thus, the term *hexavalent chromium* is a misnomer: no such substance exists. The reason for this is that chromium is a transition element and therefore tends not forming free cations, but readily combines with oxygen forming monovalent anionic complexes such as chromate (CrO_4^-) and dichromate ($Cr_2O_7^-$). In both cases chromium has an oxidation state of VI (Motzer and Guertin, 2007).

Soils

Morrison, et al. (2009) noted that UM rock-derived soils have chromium concentrations primarily contributed by chromite ($FeCr_2O_4$) and other mixed-composition spinel minerals containing chromium. These are also abundant in serpentine soils, typically occurring as magnetite-rimmed chromite. Such rims may be an alteration product of the original chromite or precipitated secondary overgrowths around the original chromite formed by the partial dissolution of iron from silicate minerals. When considering chromium weathering and dissolution in serpentine soils, magnetite rims armoring chromium-rich cores becomes important because if unmodified, such rims limit chromium dissolution during weathering.

Chromium-bearing spinel transport from UM source areas can have significant effects on chromium mobility because, when magnetite-armored rims are removed, chromite grain size decreases resulting in greater surface area, thereby increasing chromium dissolution. Additionally, lesser amounts of total chromium and nickel are associated with secondary clays and iron (hydr)oxides in both UM and serpentine soil. These secondary minerals also have high surface areas and are likely to be reactive representing the mobile fraction in water-soil interactions (Morrison, et al., 2015).

Groundwater

As described above, most naturally occurring chromium in source rocks and soil developed from these rocks generally exist as Cr(III) minerals (e.g., chromite) of which many are relatively water insoluble. However, serpentine soils, precipitation runoff in streams, and groundwater can have soluble Cr(III) cations and Cr(VI) oxyanions (**Figure 12A** from Oze (2003). That soluble Cr(II) cations exist can be seen, under standard conditions (at 25^{o}C and 1.0 bar atmospheric pressure), in the chromium-oxygen-hydrogen system as shown in the Eh-pH diagram (**Figure 12B)**: the Cr(III) stability zone occurs over a wide Eh and pH field, under both reducing to oxidizing and acid to alkaline conditions, respectively. However, under standard conditions that could predominate in groundwater, soluble chromium cations and anions may be produced from relatively insoluble Cr(III) hydroxide. Concentrations could range from 500 micrograms per liter (µg/L) to 5,000 µg/L. Under most natural groundwater conditions, such concentrations are rarely found, generally not exceeding the primary MCL of 50 µg/L for total chromium. Note that the Cr(VI) stability zone or field occurs over a much narrower range than the Cr(III) stability field. Cr(VI) species primarily occur under oxidizing (+Eh) and alkaline conditions (pH >6.0). In this field, Cr(VI) generally forms the soluble chromate (CrO_4^{2-}) oxyanion from approximately pH 7.0 to 14.0 and at an Eh from approximately –0.1 to +0.8 V (Motzer, 2017a).

The process of conversion of Cr(III) species to Cr(VI) is rather interesting, largely requiring the presence of manganese oxides to oxidize slightly soluble Cr(III) to more soluble Cr(VI). Over the last 40 years, this has been established by experimental and empirical data. The Eh-pH (redox) diagram in **Figure 13** is an example of how different manganese species form in groundwater. Solid Mn(IV) and dissolved Mn(II) species occur over a wide pH range: e.g., at a pH of ~7.5, Mn^{2+} concentrations are ~0.55 milligrams per liter or mg/L (550 µg/L) but as the pH increases above 8, solubility drops to 55 µg/L. Comparing **Figure 12A** and **12B** below, with **Figure 13**, note that the stability zones for Cr(VI) species are in similar positions as those for Mn(IV) species (Motzer, 2017b).

In California, groundwater in alluvial aquifers underlying or adjacent to UM and serpentinite source rock may contain Cr(VI) oxyanions. Geochemical conditions favoring Cr(VI) formation are the presence of (1) oxygenated water (high Eh), (2) pH ≥ 7.0, and (3) manganese oxides, particularly Mn(II) and Mn(IV) oxides. Additionally, for Cr(VI) to form, aquifer materials should be low in Fe(II), organic matter, and clays (aluminum oxides) that may be Cr(VI) adsorbents and reductants that either prevent formation of Cr(VI) or transform it back to Cr(III). Cr(VI) may also be sorbed to hydrous ferrous oxides (HFOs) occurring either coating quartz sand grains or as weathered iron oxides (e.g., hematite); these may be storage sites for Cr(VI) oxyanions. Naturally-occurring Cr(VI) in groundwater collected from wells is generally in the low µg/L (ppb) range. However, U.S. Geological Survey studies have determined that 4.5 percent of 918 sampled wells had Cr(VI) exceeding the former California maximum contaminant level (MCL) of 10 ppb[†] (Motzer, 2005; Oze, et al., 2007; Izbicki, et al.,2015).

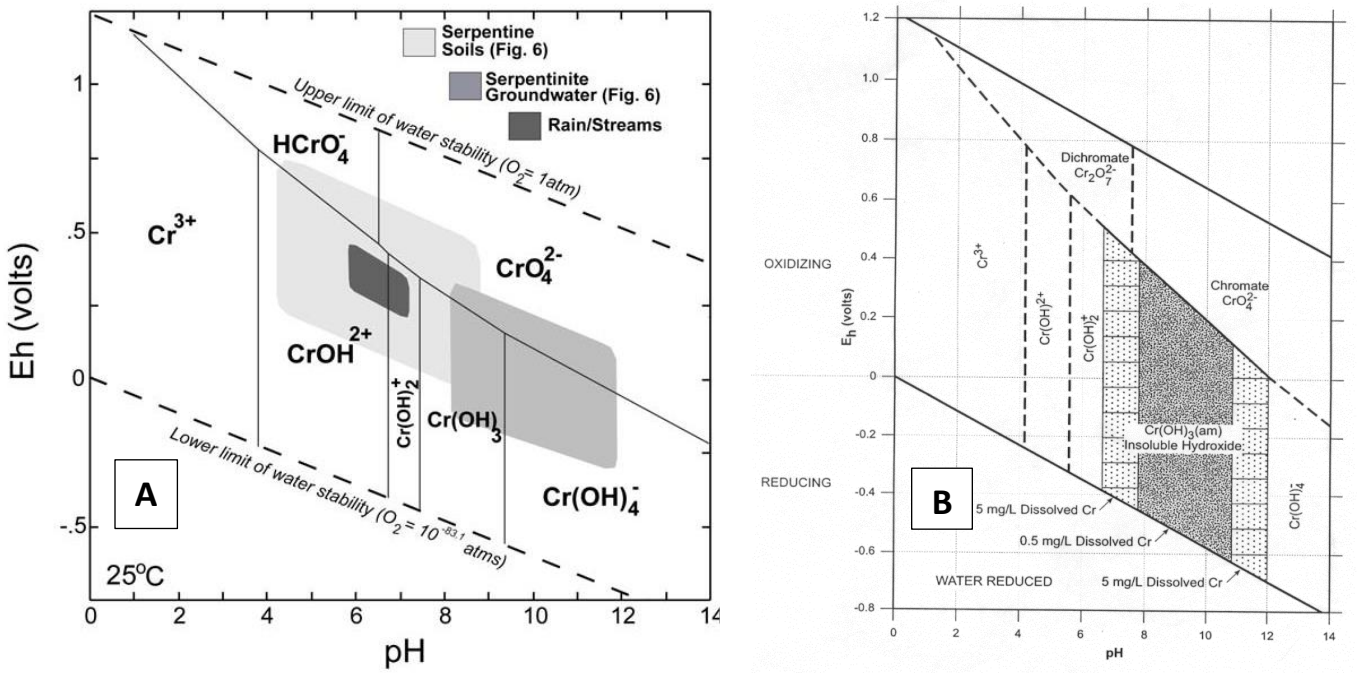

Figure 12A*: Eh-pH stability diagram from Oze (2003) showing possible ranges for Cr(III) and Cr(VI) formation and occurrence in serpentinite soils, groundwater, and streams.* ***Figure 12B****: Eh-pH diagram with stability diagram showing possible amounts of dissolved soluble Cr(III) in water (Hem, 1989).*

[†] On May 31, 2017, the Sacramento County Superior Court issued a judgement invalidating the Cr(VI) MCL, siding with the plaintiffs that the State Water Resource Control Board (SWRCB) had not taken economic considerations into account when establishing the MCL. The court also ordered that the SWRCB adopt a new Cr(VI) MCL. On August 1, 2017, the SWRCB decided not to appeal this decision but rather reopen the MCL process to establish a new MCL and they've indicated that this may take several years. Therefore, until a new primary MCL is determined for Cr(VI) the total Cr primary MCL of 50 µg/L, which includes both Cr(III) and Cr(VI), will be used by California water districts and suppliers.

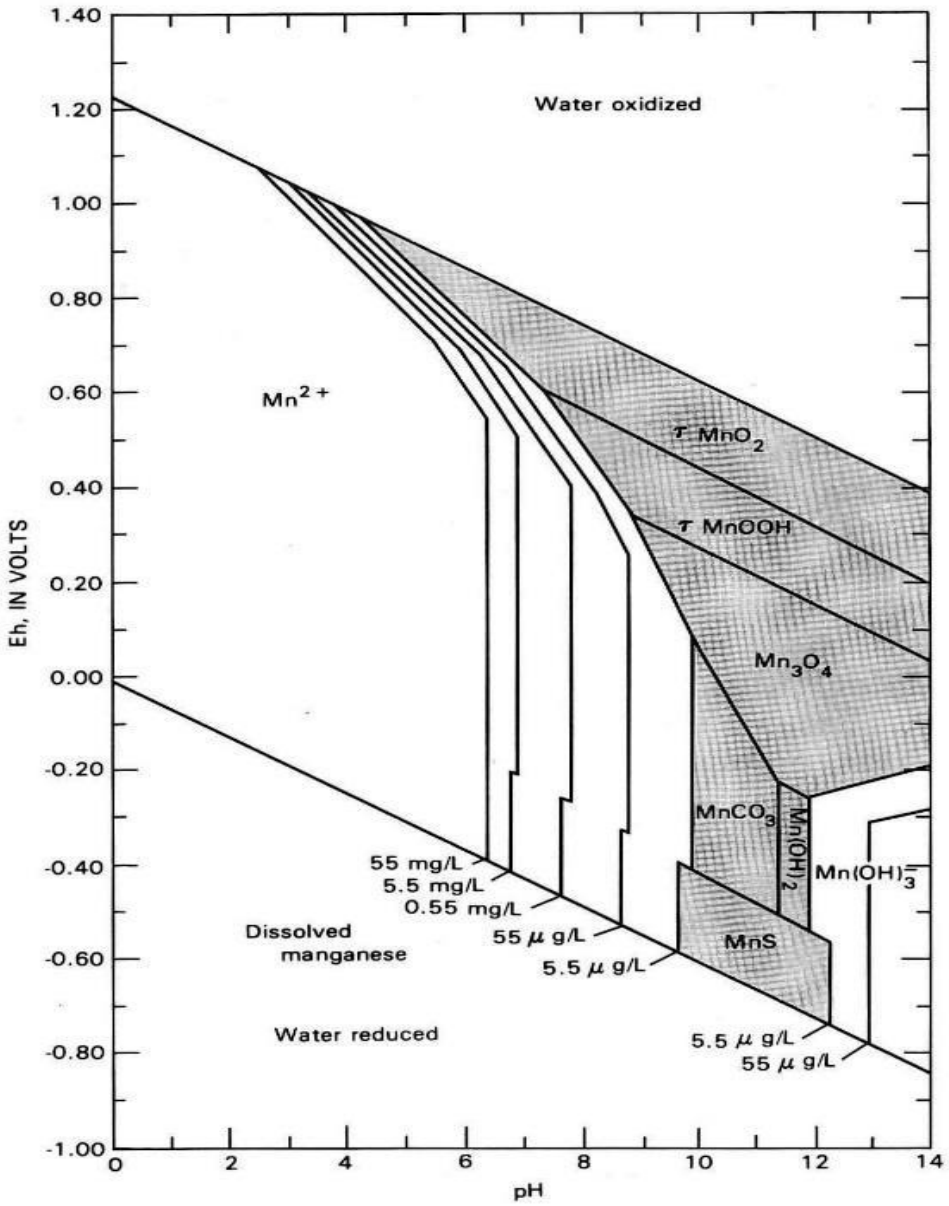

Figure 13: *Eh-pH stability diagram for manganese (Mn) in the system Mn-O-C-S at 25^{o} C and 1 atmosphere pressure. Solid manganese species are highlight in gray (Hem, 1989).*

Manganese oxides occurring as insoluble manganese minerals such as birnessite "catalyze" and oxidize Cr(III) species. Birnessite and other δMnO_2 minerals in particulate form tend to sorb cations because they have negative surface charges (see **Figure 14**). Once oxidized, hydrous ferrous oxides (HFOs) such as ferrihydrite (generally $FeOOH \bullet nH_2O$) particles become the predominant sorptive substances for complex oxyanions such as CrO_4^{2-} because these HFOs have positive surface charges. Therefore, HFOs likely act as "storage" sites for Cr(VI) oxyanions. This is important because as infiltrating water percolates downward through the unsaturated zone it tends to "remobilize" the sorbed Cr(VI), which then accumulates in groundwater.

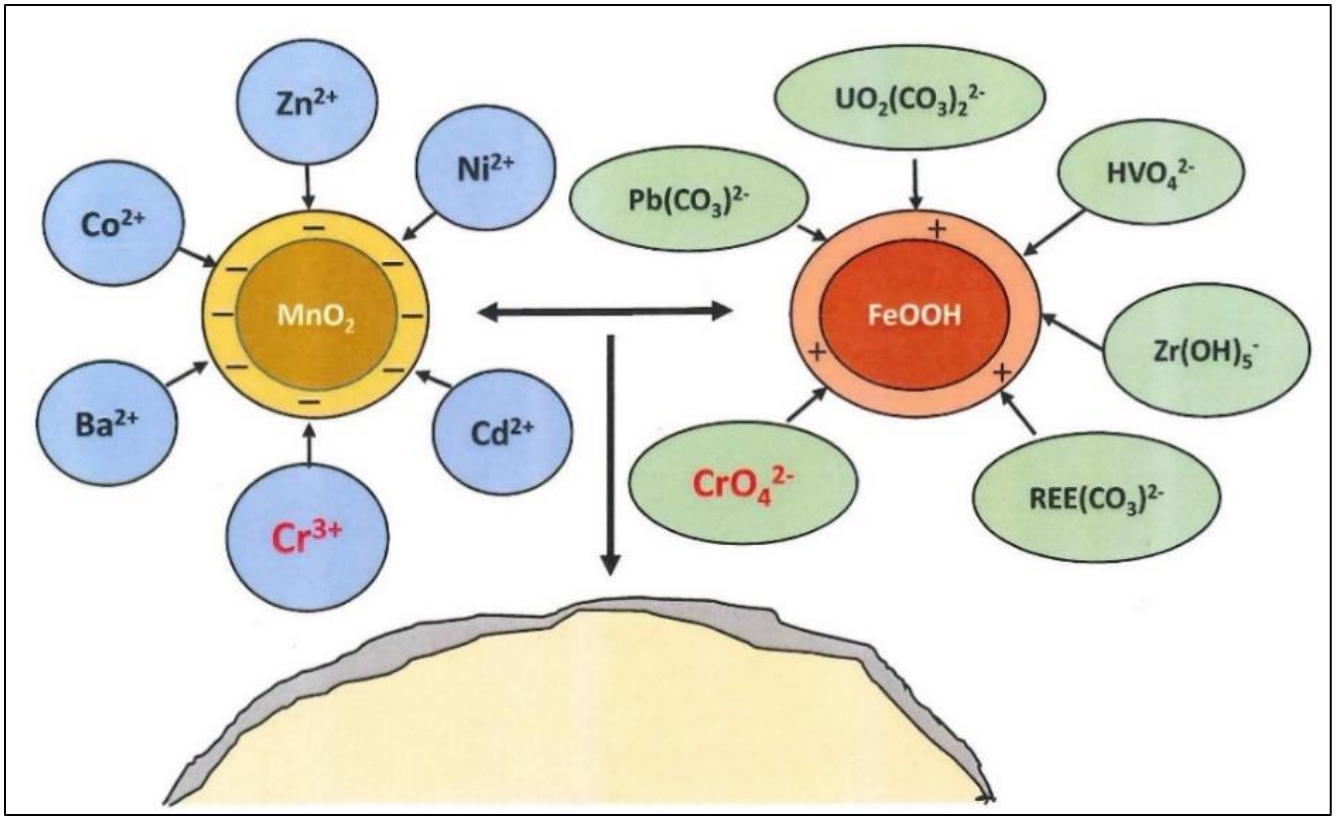

***Figure 14**: Electrochemical model for sorption of soluble cations ("blue" circles on left) to MnO_2 with formation of Cr(VI) oxyanion species such as CrO_4^{2-} ("green" ovals on right) and subsequent sorption on ferrihydrite (FeOOH). Sorption of cations and oxyanions is generally restricted to particle surfaces which may occur at nanometer scales. Diagram modified after Koschinsky and Hein (2017) in Motzer,2017b).*

Field Trip Stops

Only six major field trip stops are shown in this field guide. We will make additional minor stops as needed (e.g. for views, “arm waving, “etc.).

Stop 1: *Phyllis Ellman trailhead at the start of the hike. The trail traverses a large landslide encompassing rock rubble consisting of various rock types that will be observed in place at higher elevations in the exotic block terrain. April 2016 photo.*

***Stop 2**: Top photo: ancestral Native American Coastal Miwok mortar hole in garnet blueschist "slab/boulder" in landslide area. Bottom photo: Close-up view of euhedral garnets. October 2017 photos.*

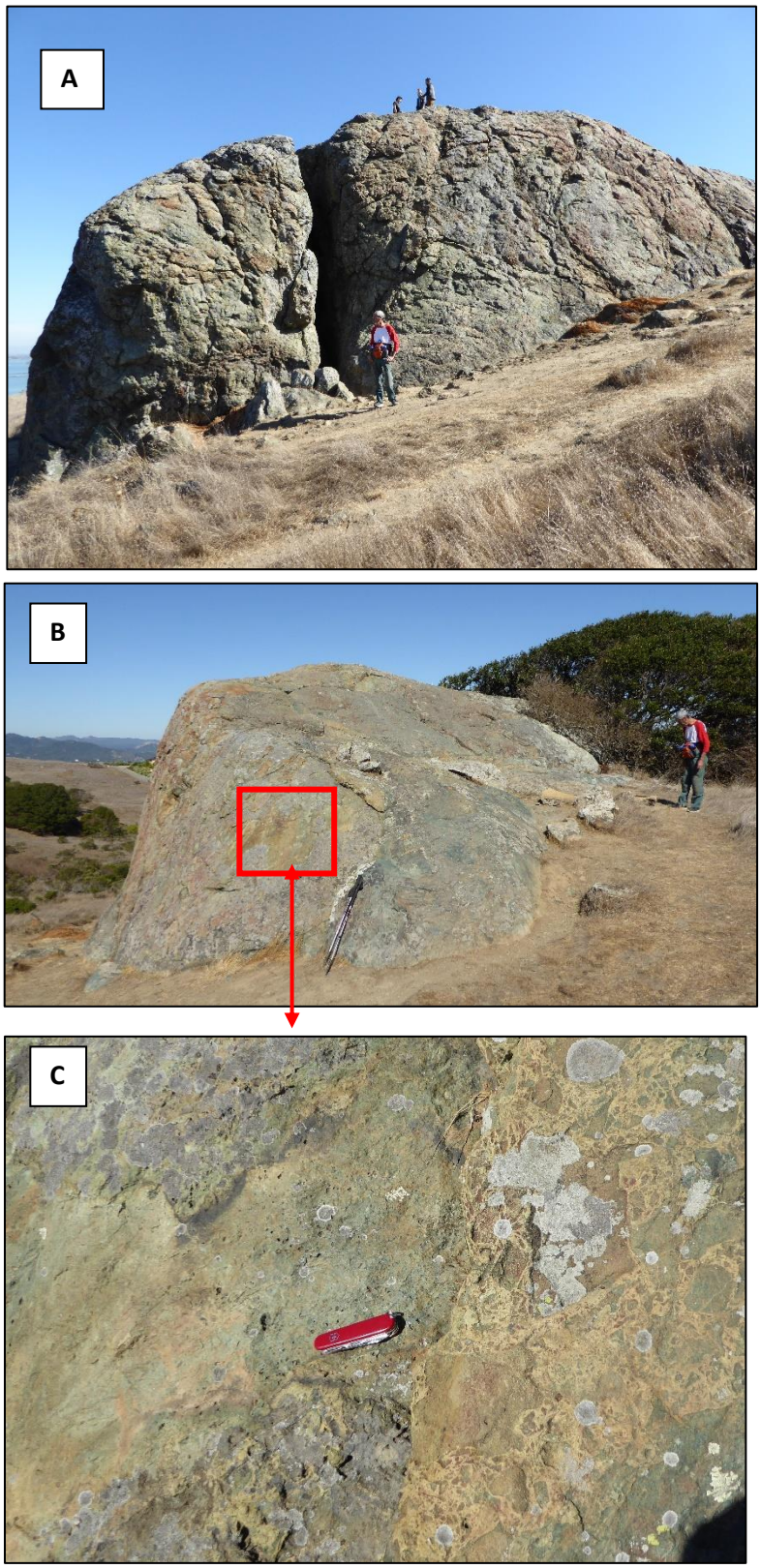

Stop 3: *Climbing Rock: Consisting of felsic metavolcanics (Wakabayashi, 2017).* ***A:*** *view east. Large fracture used by locals to practice freehand and rope-supported climbing.* ***B****: view north. Mark Petrofsky for scale.* ***C****: closeup of remnant hydrothermal explosion breccias and pillow basalt structures. October 2017 photos*.

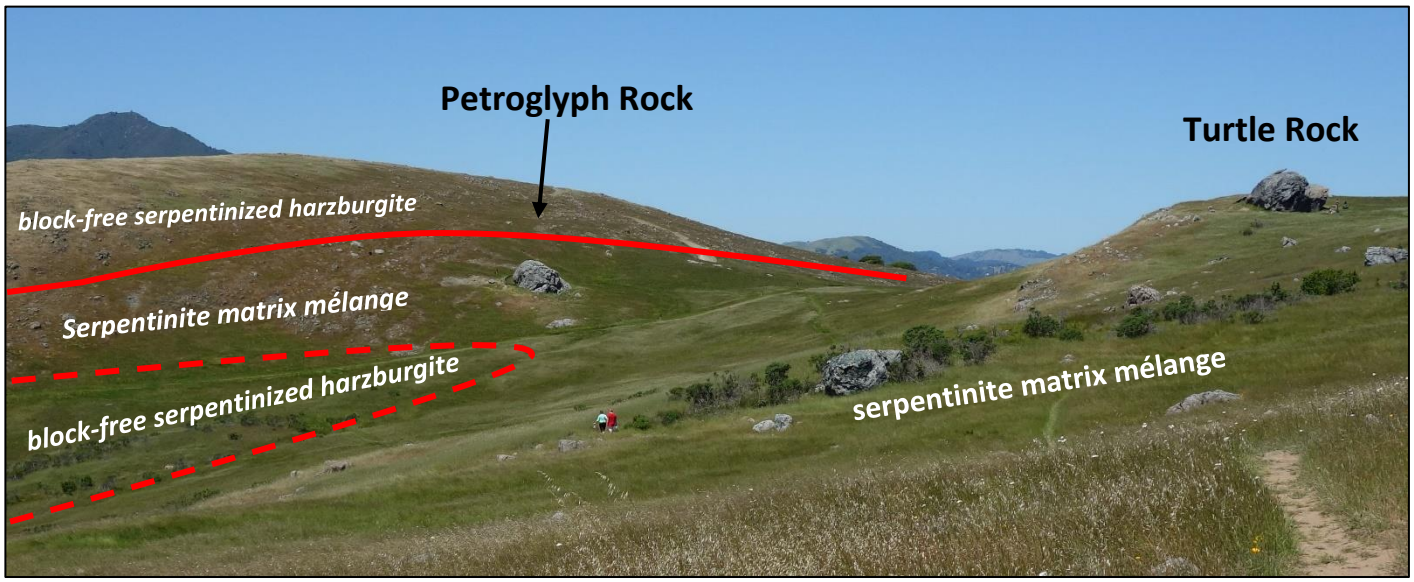

*Panorama view of **Stop 4**: Turtle Rock and **Stop 5:** Petroglyph Rock. View northward with Mount Tamalpais in background on left side of photo.*

***Stop 4A**: Turtle Rock. Garnet amphibolite overprinted by blueschist (Wakabayashi, 2013). AIPG U.C. Davis and Sonoma State University students for scale. **B:** Close-up view of tight, imbricate folding. May 2017 photos.*

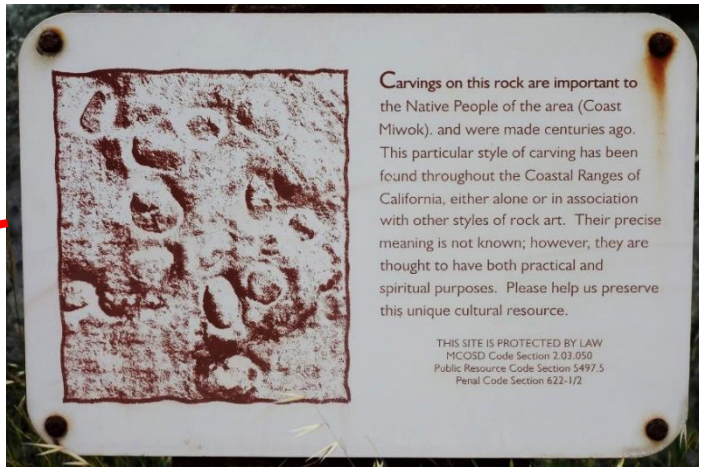

***Stop 5A**: Petroglyph Rock with petroglyphs carved by ancestral Miwok Native Americans. Rock outcrop composed of relatively erosion resistant garnet blueschist/eclogite exotic block in weathered serpentinite matrix mélange (see Wakabayashi, 2017). April 2016 photo.*

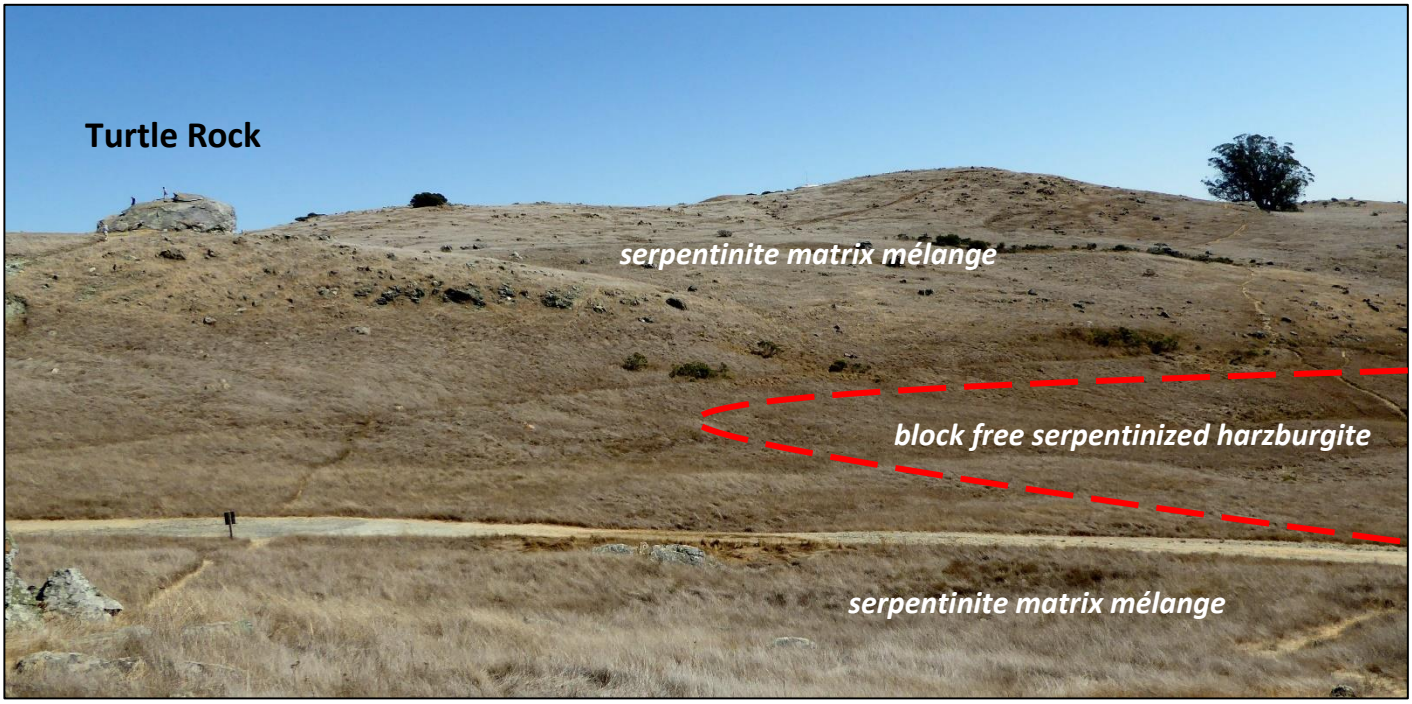

***Stop 5B:** View eastward from Petroglyph Rock back toward Turtle Rock. Exotic blocks in serpentinite terrain with underlying serpentinite-lacking exotic blocks (Wakabayashi, 2013). The two "units" are most likely separated by thrust faults (looking into the thrust in upper red line – see Bero, 2014). October 2017 photo. (Reverse direction from **Stop 4** photo above.)*

*View northward toward and approaching "Serpentinite Quarry" (see **Stop 6** below) with old redwood water tanks, now replaced with new tank. May 2015 photo.*

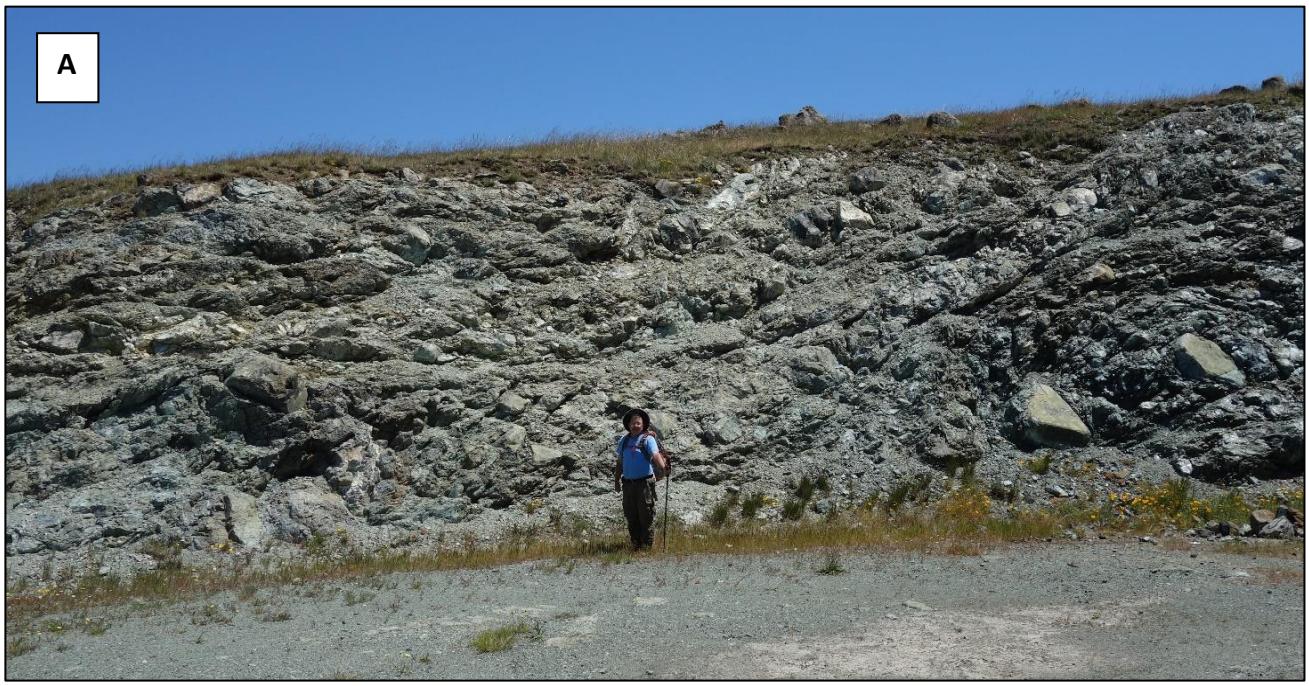

***Stop 6A**: Serpentinite Quarry. Exposed rock consisting largely of serpentinized harzburgite. Note low-angle shearing in the quarry wall consistent with "regional" east-west thrusting. John Christian posing for scale.*

***B:** Secondary or weathered "vein" deposit of magnesite ($MgCO_3$). Pocket knife for scale.*

***C:** Secondary(?) magnetite (Fe_3O_4 – inside red circle) derived from serpentinite rock/soil, possible biproduct of chromite ($FeCr_2O_4$) decomposition. 6A and 6B: April 2016 photos and 6C: October 2017 photo.*

Annotated Bibliography and References Cited

History:

Hogan, C.M., 2008, *Ring Mountain – Carving in United States in The West*: The Megalithic Portal: http://www.megalithic.co.uk/article.php?sid=19244.

Marin Conservation League, 2011, *Walk Into History #8 Ring Mountain*: http://www.marinconservationleague.org/images/stories/pdfs/events/wh11b_programweb.pdf.

Ecology: Endemic Vegetation (Flowers and Grasses), Butterflies, Birds, etc.:

Anacker, B.L., 2014, *The Nature of Serpentine Endemism:* American Journal of Botany, v.101, n. 2, pp.219-224.

Elder, W., 2013, *Geology of the Golden Gate Headlands*: Northern California Geological Society (NCGS) Field Trip Guide, Saturday, June 22nd, 18 p.

Six photos of rare and endangered plants living on Presidio serpentine soils and dunes.

Marin County Parks.org (2010):

Field Guides: http://www.marincountyparks.org/depts/pk/divisions/open-space/main/fieldguides

Ring Mountain Open Space Preserve: https://www.marincountyparks.org/~/media/images/departments/pk/open-space/ring-mountain/17_ringmtn-121314w.pdf

Oze, C.J., LaForce, M.J., Wentworth, C.M., Hanson, R.T., Bird, D.K., ad Coleman, R.G., 2002, *Chromium Geochemistry of Serpentinous Sediment in the Willow Core, Santa Clara County, CA*: U.S. Geological Survey Open File Report 03-251, 9 p. with figures and tables.

Oze, C., Skinner, C.X., Schroth, A.W., and Coleman, R.C., 2008, *Growing up Green on Serpentine Soils: Biogeochemistry of Serpentine Vegetation in the Central Coast Range of California*: Applied Geochemistry, v. 23, pp. 3391-3403.

Geology Field Guides and Geology/Geochemistry Papers:

Alden, Andrew, 2011, *Geological Outings Around the Bay: Ring Mountain*: http://science.kqed.org/quest/2011/05/19/geological -outings-around-the-bay-ring-mountain/

General introductory geology of Ring Mountain with photos.

Bebout, G.E., Scholl, D.W., Stern, R.J., Wallace, L.M., and Agard, P., 2018, *Twenty Years of Subduction Zone Science: Subduction Top to Bottom 2 (ST2B-2)*: GSA Today, v. 28, n.2, pp. 4-10.

Bero, D., 2013, *Geology of Ring Mountain and Tiburon Peninsula, Marin County, California*: Geological Society of America Abstracts with Programs, v. 46, n. 6, p.69, 16 p. https://gsa.confex.com/gsa/2013CD/webprogram/Paper218964.html

Bero, D.A., unknown date, *Fault-related Metamorphism along a Remnant of the Coast Range Thrust, Ring Mountain, Marin County*, California, 15 p. http://www.es.ucsc.edu/~crowe/structure/handouts/XTRA_Bero_Rowe_05.pdf.

Butler, J.P., Beaumont, C., and Jamieson, R.A., 2014, *The Alps 2: Controls on Crustal Subduction and (Ultra)High-pressure Rock Exhumation in Alpine-type Orogens*: Journal. Geophysical Research Solid Earth, v. 119, pp. 5987–6022; DOI: 10.1002/2013JB010799.

Animated models showing subduction and obduction of metamorphic rocks.

Day, D., 2004, *The Finer Points of Subduction on the Tiburon Peninsula*: http://www.ncgeolsoc.org/Field%20Trips/2004%20-%202005/Tiburon%20Peninsula%20FT/TiburonPeninsulaFT.htm

Summary of Northern California Geological Society field trip to Ring Mountain with field trip leader David Bero.

Dilek, Y. and Furnes, H., 2014, *Ophiolites and Their Origins*: Elements, v, 10, n. 2, pp. 93–100.

Ernst, W.G., 1988, *Tectonic History of Subduction Zones Inferred from Retrograde Blueschist P-T Paths*: Geology, v. 16, p. 1081–1084.

Evans, B., Hattori, K., and Baronnet, A., 2013, *Serpentinite, What, Why, Where?*: Elements, v. 9, n. 2, pp. 107-113.

Feighner, M., 2006, *Metamorphic Rocks of Ring Mountain, Tiburon:* Physical-Science Review, v. 1, May issue, http//mathsci.solano.edu/users/mfeighne/vol1.page2.htm.

Polarized light photomicrographs of amphibolite, blue schist, serpentinite and eclogite collected from Ring Mountain.

Gordon, E., 2005 (updated 2005 by Detterman, M. and Garbutt, P.M.), *Blueschists and Breweries: Brewschist II*: Northern California Geological Society Field Trip Guide, June 25-26, 2005: http://norcalgeol.site.aplus.net/Field%20Trips/Brewschist2FTJune05/Blueschist%20II.htm.

Guillot, S. and Hattori, K., 2013, *Serpentinites: Essential Roles in Geodynamics, Arc Volcanism, Sustainable Development, and the Origin of Life*: Elements, v. 9, n. 2, pp. 95–98.

Hirth, G. and Guillot, S., 2013, *Rheology and Tectonic Significance of Serpentinite*: Elements, v. 9, pp. 107-113.

Role of serpentinite strike-slip faulting and subduction. Figure 6 describes distribution of serpentinite in central California. Figure 7 is a schematic diagram of subduction-related serpentinite.

MacKinnon T. C., 2018, *Early Accretionary History of the Franciscan Complex as inferred from the Yolla Bolly/Black Butte Area of the Eastern Belt*: abstract and presentation: Northern California Geological Society March 2018 Newsletter, www.ncgeolsoc.org/

Mulcahy, S.R., King, R.L., and Vervoot, J.D., 2009, *Lawsonite Lu-Hf Geochronology: A New Geochronometer for Subduction Zone Processes*: Geology, v. 37, pp. 987-990.

Raymond, L.A., 2017, *What is Franciscan?: Revisited*: International Geology Review, 63 p., DOI: 10.1080/00206814.2017.1396933.

Extensive, comprehensive, and current review of the Franciscan Complex.

Saha, A., Basu, A.R., Wakabayashi, J., and Wortman, G.L., 2005, *Geochemical Evidence for Subducted Infant Arc in Franciscan High-Grade Metamorphism Tectonic Blocks*: Geological Society of America Bulletin, v. 117, n. 9-10, pp. 1318-1335.

Sloan, D, and Karachewski, J., 2006, *Geology of the San Francisco Bay Region*: California Natural History Guides, University of California Press, Berkeley, CA, 335 p.

Excellent generalized San Francisco Bay area geology and photos. Brief RMOSP geology description on pages 104-105.

Stoffer, P., 2002, Rocks and Geology in the San Francisco Bay Region: U.S. Geological Survey (USGS) Bulletin 2195, USGS, Reston, VA, 58 p., http://geopubs.wr.usgs.gov/bulletin/b2195.

Introduction to Bay area rocks and geology including rock specimen photos and descriptions of metamorphism and associated rocks.

Templeton, A.S., 2011, *Geomicrobiology of Iron in Extreme Environments*: Elements, v.7, pp. 95-100.

Vogt, K. and Gerya, T., 2014, *Deep Plate Serpentinization Triggers Skinning of Subducting Slabs*: Geology, v. 42, n. 8, PP.723-726.

Wakabayashi, J., 2001, *Blueschists and Microbreweries of Coastal Northern California: Two Subjects of International Fame*: Northern California Geological Society Field Trip Guide for *The Golden B.E.A.R Tour 2001 (Blueschists, Eclogites, Amphibolites, Refreshments)*, 9 p. with figures.

Wakabayashi, J., 2005, *Blueschists and Breweries – Blueschists II A Tour of Fine Rocks and the west Coast Brewing Art:* NCGS Field Trip Guide June 25, and June 26, 2005, 16 p.

Wakabayashi, J., 2013, *Subduction Initiation, Subduction Accretion, and Non-Accretions, Large-Scale Material Movement, and Localization of Subduction Megaslip Recorded in Franciscan Complex and Related Rocks, California*: Geological Society of America Field Guide 32, pp. 129-161.

Stop 4: Ring Mountain, Tiburon Peninsula, Taylor Avenue Parking contains detailed Ring Mtn. geologic map (Figure 17).

Wakabayashi, J., 2017, *Structural Context and Variation of Ocean Plate Stratigraphy, Franciscan Complex, California: Insight into Mélange Origins and Subduction Zone Processes*: Progress in Earth and Planetary Science, v. 4, n. 18, 23 p.

Updated and expanded version of Wakabayashi and Rowe 2015 publication with colorized Ring Mountain geologic map.

Wakabayashi, J. and Dumitru, T.A., 2007, *$^{40}Ar/^{39}Ar$ Ages from Coherent, High-Pressure Metamorphic Rocks of the Franciscan Complex, California: Revisiting the Timing of Metamorphism of the World's Type Subduction Complex*: *International Geology Review*, v. 49, p. 873–906.

Wakabayashi, J. and Rowe, C.D., 2015, *Whither the Megathrust? Localization of Large-Scale Subduction Slip along the Contact of a Mélange*: International Geology Review, v. 57, nos. 5 – 8, pp. 854-870.

Figure 1 contains a location map of San Francisco Bay area Franciscan Complex geology and structure.

Detailed Geologic/Soil Maps:

Bero, David A., 2014*, Geology of Ring Mountain and Tiburon Peninsula, Marin County, California*: California Geologic Survey (CGS) Map Sheet 62, CGS, Sacramento, CA.

Recent geologic mapping presented in two detailed map sheets of Ring Mountain and the Tiburon Peninsula with accompany descriptive text.

Churchill, R.K. and Hill, R.L., 2000, *A General Location Guide for Ultramafic Rocks in California – Areas More Likely to Contain Naturally Occurring Asbestos*: California Geological Survey Open File Report and map (1: 1,100,000).

U.S. Department of Agriculture (USDA), 2016, *Soil Survey Maps*: http://websoilsurvey.sc.egov.usda.gov/App/WebSoilSurvey.aspx.

The Critical Zone: Soil and Sediment:

Kashiwagi, J.H., 1985, *Soil Survey of Marin County, California*: U.S. Department of Agriculture (USDA), Soil Conservation District, 243 p.

Kruckeberg, A.R., 1984, *California Serpentinites: Flora, Vegetation, Geology, Soils, and Management Problems*: University of California Press, Ltd., Berkeley, CA, 168 p.

Kruckeberg, A.R., 2006, *Introduction to California Soils and Plants: Serpentine, Vernal Pools, and Other Geobotanical Wonders*: University of California Press, Berkeley, CA, 280 p.

Kumar, A., Maiti, S.K., 2013, *Availability of Chromium, Nickel and other Associated Heavy Metals of Ultramafic and Serpentine Soil/Rock and in Plants*: International Journal of Emerging Technology and Advanced Engineering, v. 3, issue 2, pp. 256-268.

Morrison, J.M., Goldhaber, M.B., Mills, C.T., Breit, G.N., Hooper, R.L., Holloway, J.M., Diehl, S.F., and Ranville, J.F., 2015, *Weathering and Transport of Chromium and Nickel from Serpentine in Coast Range Ophiolite to the Sacramento Valley, California, USA*: Applied Geochemistry, v. 61, pp. 72-86.

Chromium and Manganese Geochemistry:

Hansel, C.M., Ferdelman, T., and Tebo, B.M., 2015, *Cryptic Cross-Linkages among Biogeochemical Cycles: Novel Insights from Reactive Intermediates*: Elements Magazine, v. 11, pp. 409-414.

Hem J.D., 1989 (third edition), *Study and Interpretation of the Chemical Characteristics of Natural Water:* U.S. Geol. Survey Water Supply Paper 2254, USGS, Alexandria, VA, 263 p.

Izbicki, J.A., Wright, M.T., Seymour, W.A., McCleskey, R.B., Fram, M.S., Belitz, K., and Esser, B.K., 2015, *Cr(VI) Occurrence and Geochemistry in Water from Public Supply Wells in California*: Applied Geochemistry, v.63, pp. 203-217.

Koschinsky, A. and Hein, J.R., 2017, *Marine Ferromanganese Encrustations: Archives of Changing Oceans*: Elements Magazine, v. 13, n. 3, pp. 177–182.

Morrison, J.M., Goldhaber, M.B., Lee, L., Holloway, J.M., Richard B. Wanty, J.B., Wolf, R.E., Ranville, J.F., 2009, *A Regional-scale Study of Chromium and Nickel in Soils of Northern California, USA*: Applied Geochemistry, v.24, pp. 1500–1511.

Motzer, W.E., 2005*, Chemistry, Geochemistry, and Geology of Chromium and Chromium Compounds (Chapter 2)*, in J. Guertin, J.A. Jacobs, and CP. Avakian (editors), *Chromium(VI) Handbook* – Independent Environmental Technical Evaluation Group (IETEG)*,* CRC Press, Boca Raton, FL, pp. 23-91.

Motzer, W.E., 2017a, *Toxic Terra – Part 10 (Chromium):* The Vortex*,* v. LXXIX, n. 6, pp. 6-7, www.calacs.org.

Motzer, W.E., 2017b, *Toxic Terra – Part 11 (Chromium):* The Vortex*,* v. LXXIX, n. 7, pp. 6-7, www.calacs.org.

Motzer, W.E. and Guertin, J., 2007, *"Valencing" Oxidation States: A Legacy of Erin Brockovich*: The Vortex, v. LXVIII, n. 8, pp. 5 and 7, www.calacs.org.

Oze, C., 2003, *Chromium Geochemistry of Serpentinites and Serpentine Soils:* Stanford University Doctoral dissertation, 198 p.

Oze, C., Bird, D.K., and Fendorf, S., 2007, *Genesis of Hexavalent Chromium from Natural Sources in Soil and Groundwater*: Proceedings of the National Academy of Sciences (PNAS), v. 104, n. 16, pp. 6544–6549**.**

Priestaf, M.J. and Rednock, D., 2015, *An Electrochemical Study of Chromium Oxidation by Manganese Oxides*: Geological Society of America Abstracts with Programs, v. 47, n.7, pp. 301, https://gsa.confex.com/gsa/2015AM/webprogram/Paper269901.html.

Snyder, W.S., 1978, *Manganese Deposited by Submarine Hot Springs in Chert-Greenstone Complexes, Western United States*: Geology, v. 6, pp. 741-744.

Taliaferro, N.L., and Hudson, F.S, 1943, *Genesis of the Manganese Deposits of the Coast Ranges of California*, in *Manganese in California*: California State Division of Mines (CSDM) Bulletin No. 125, CSDM, Ferry Building, San Francisco, pp. 217-275.

Trask, P.D., Wilson, I.F. and Simons, F.S.,1943, *Manganese Deposits of California: A Summary Report*, in *Manganese in California*: California State Division of Mines (CSDM) Bulletin No. 125, CSDM, Ferry Building, San Francisco, pp. 51-216.

Acknowledgements

The authors would like to thank:

Ron and Sara Van Dette, with the Contra Costa Hills Hiking Club, who originally led several hikes into RMOSP.

John Christian, our friend and colleague, who pointed out many interesting sites within RMOSP including petroglyphs, flowers, minerals, and interesting mineralized outcrops.

Dr. Will Schweller, Past NCGS President and current Field Trip Coordinator who encouraged us to develop and conduct this field trip. His edits and suggestions greatly improved the text.

Dr. Tom MacKinnon who graciously provided references, slides, and photos.

All photos unless otherwise noted by Bill Motzer.

Trail map overlay on RMOSP (Figure 8) by Mark Petrofsky.